Three-Dimensional Reconstruction of Thin Filaments Containing Mutant Tropomyosin

M. Rosol,* W. Lehman,* R. Craig,† C. Landis,‡ C. Butters,‡ and L. S. Tobacman‡

*Department of Physiology, Boston University School of Medicine, Boston, Massachusetts 02118; †Department of Cell Biology, University of Massachusetts Medical School, Worcester, Massachusetts 01655; and ‡Departments of Internal Medicine and Biochemistry, The University of Iowa College of Medicine, Iowa City, Iowa 52242 USA

ABSTRACT Interactions of the components of reconstituted thin filaments were investigated using a tropomyosin internal deletion mutant, D234, in which actin-binding pseudo-repeats 2, 3, and 4 are missing. D234 retains regions of tropomyosin that bind troponin and form end-to-end tropomyosin bonds, but has a length to span only four instead of seven actin monomers. It inhibits acto-myosin subfragment 1 ATPase (acto-S-1 ATPase) and filament sliding in vitro in both the presence and absence of Ca^{2+} (Landis et al., 1997, *J. Biol. Chem.* 272:14051–14056) and lowers the affinity of S-1·ADP for actin while increasing its cooperative binding. Electron microscopy and three-dimensional reconstruction of reconstituted thin filaments containing actin, troponin, and wild-type or D234 tropomyosin were carried out to determine if Ca^{2+}-induced movement of D234 occurred in the filaments. In the presence and absence of Ca^{2+}, the D234 position was indistinguishable from that of the wild-type tropomyosin, demonstrating that the mutation did not affect normal tropomyosin movement induced by Ca^{2+} and troponin. These results suggested that, in the presence of Ca^{2+} and troponin, D234 tropomyosin was trapped on filaments in the Ca^{2+}-induced position and was unable to undergo a transition to a completely activated position. By adding small amounts of rigor-bonded *N*-ethyl-maleimide-treated S-1 to mutant thin filaments, thus mimicking the myosin-induced "open" state, inhibition could be overcome and full activation restored. This myosin requirement for full activation provides support for the existence of three functionally distinct thin filament states (off, Ca^{2+}-induced, myosin-induced; cf. Landis et al., 1997; Vibert et al., 1997, *J. Mol. Biol.* 266:8–14). We propose a further refinement of the three-state model in which the binding of myosin to actin causes allosteric changes in actin that promote the binding of tropomyosin in an otherwise energetically unfavorable "open" state.

INTRODUCTION

Skeletal muscle activity is regulated sterically by tropomyosin strand movement blocking and unblocking myosin-cross-bridge binding sites on actin filaments. Tropomyosin thereby controls cross-bridge cycling and, consequently, contraction (Haselgrove, 1972; Huxley, 1972; Parry and Squire, 1973; Lehman et al., 1994; Holmes; 1995). Tropomyosin is a modular protein containing seven successive quasi-repeating amino acid sequences believed to associate with seven corresponding axially adjacent actin monomers on filamentous actin (F-actin), causing the protein to lie longitudinally along the long-pitch actin helix (McLachlan and Stewart, 1976; Phillips et al., 1986). Elongated tropomyosin molecules bind end to end on actin to form long, continuous strands (Flicker et al., 1982). The resulting axial continuity of the tropomyosin strand allows cooperative azimuthal movement between switched-on and switched-off locations on filaments under the influence of troponin and Ca^{2+}. Huxley and others proposed a two-state steric model of muscle regulation based on this apparent "on-off" switching (Huxley, 1972; Haselgrove, 1972; Parry and Squire, 1973). However, the two-state model failed to explain how tropomyosin, as a simple steric inhibitor, also potentiated actin-myosin interaction after Ca^{2+} activation (Bremel et al., 1972; Murray and Weber, 1973). Study of the kinetics of muscle activation (Lehrer and Morris, 1982; McKillop and Geeves, 1993; Lehrer, 1994; Landis et al., 1997; Lehrer and Geeves, 1998) and recent structural evidence (Holmes, 1995; Poole et al., 1995; Vibert et al., 1997) have led to a new model in which tropomyosin moves between three, not two, distinct states. Full switching on of filaments by reversal of steric blocking is thought to occur stepwise, requiring first a movement of tropomyosin caused by Ca^{2+} binding to troponin, followed by a further movement induced by myosin binding to actin. Ca^{2+} activation leads to a 25° azimuthal movement of tropomyosin around the thin filament, which uncovers most but not all of the strong myosin-binding sites on actin (Lehman et al., 1994; Poole et al., 1995; Vibert et al., 1997; Xu et al., 1999). Filaments decorated with myosin subfragment 1 (S-1) show a small, additional ~10° movement of tropomyosin that exposes the entire myosin-binding interface and permits full activation (Vibert et al., 1997).

To be consistent with an activation process in which both Ca^{2+}- and myosin-induced movements are required, tropomyosin in the Ca^{2+}-induced position should sterically inhibit the binding of cross-bridges, although to a lesser extent than in the absence of Ca^{2+} (Vibert et al., 1997). Hence, a troponin-tropomyosin complex that permits Ca^{2+}-induced movement but not myosin-induced movement would inhibit myosin cycling. Filaments with a tropomyosin deletion mu-

Received for publication 22 July 1999 and in final form 22 October 1999.

Address reprint requests to Dr. William Lehman, Department of Physiology, Boston University School of Medicine, 80 East Concord Street, Boston, MA 02118. Tel.: 617-638-4397; Fax: 617-638-4273; E-mail: lehman@med-rana.bu.edu.

0006-3495/00/02/908/10 $2.00

tant, D234, in which actin binding pseudo-repeats 2, 3, and 4 are missing, appeared to behave in this way when assessed functionally (Landis et al., 1997). Despite the fact that it bound normally to actin and troponin, D234 conferred inhibition on actomyosin ATPase and filament sliding in vitro that was not reversed by Ca^{2+} and troponin (Landis et al., 1997), raising the possibility that tropomyosin was trapped in the Ca^{2+} position and myosin-induced movement was not possible or was incomplete. This possibility was tested directly here, using the mutant tropomyosin. Electron microscopy and 3D-image reconstruction show that D234 tropomyosin shifts in position normally on actin in response to Ca^{2+}. The inhibition of actomyosin ATPase and filament sliding suggests that D234 is unable to move to the fully switched-on position in the presence of myosin and ATP. However, this inhibition is overcome by the addition of strongly bound myosin heads. These results are consistent with activation representing a progression between states rather than a simple switch. Based on previously presented and new kinetic data, we propose a refinement of the three-state model of the thin filament to include allosteric changes in actin that enhance the binding of tropomyosin in the myosin-induced state.

MATERIALS AND METHODS

Protein preparation

Wild-type rat striated muscle α-tropomyosin and mutant α-tropomyosin with residues 49–167 deleted (D234 tropomyosin) were expressed as previously described (Landis et al., 1997) in *Escherichia coli* with a dipeptide (Ala^1-Ser^2) at the N-terminus to ensure actin binding and polymerization (Monteiro et al., 1994). The mutant possesses four of the seven quasi-repeating regions (1, 5, 6, and 7) of the molecule in tandem, with intervening regions 2, 3, and 4 deleted. The recombinant tropomyosin was purified according to the method of Willadsen et al. (1992), as modified by Landis et al. (1997). Bovine cardiac tropomyosin and troponin (Tobacman and Adelstein, 1986), rabbit skeletal muscle F-actin (Spudich and Watt, 1971), tropomyosin (Cohen and Cohen, 1972), and fast muscle myosin S-1 (Weeds and Taylor, 1975) were purified as previously described from tissue homogenates. *N*-Ethyl-maleimide (NEM) modification of myosin S-1 was carried out by adding [^{14}C]NEM to S-1 in a 10:1 molar excess, using the labeling procedure described previously (Williams et al., 1988).

Electron microscopy and helical reconstruction

Thin filaments were reconstituted by combining 40 μM F-actin, 20 μM D234 tropomyosin, and 20 μM troponin in solution consisting of 10 mM sodium phosphate (pH 7.0), 5 mM $MgCl_2$, 1 mM dithiothreitol, 1 mM ATP, and either 0.5 mM EGTA or 0.1 mM Ca^{2+}. Actin-tropomyosin controls, lacking troponin, were produced by combining 25 μM F-actin and high amounts of tropomyosin (25–50 μM) in the above buffer at 100 mM NaCl to guarantee tropomyosin binding (particularly that of D234) under electron microscopic (EM) conditions. All samples were left to incubate at room temperature for ~15 min before dilution with additional buffer to 0.5–1.0 μM actin before application to carbon-coated electron microscope grids. Grids were then negatively stained with 1% uranyl acetate as previously described (Moody et al., 1990). Electron micrograph images were recorded at 60,000× magnification under low-dose conditions (~12 $e^-/Å^2$) on a Philips CM120 electron microscope. Micrographs were digitized using an Eikonix model 1412 CCD camera at a pixel size corresponding to ~7.0 Å in the filaments (Vibert et al., 1993). Regions of filaments suitable for helical reconstruction were selected on the basis of filament straightness, lack of aggregation, and uniformity of staining. Slightly curved filaments were straightened by applying spline-fitting algorithms (Egelman, 1986). Helical reconstruction was carried out by standard methods (DeRosier and Moore, 1970; Amos and Klug, 1975; Owen et al., 1996), as previously described (Vibert et al., 1993, 1997). Statistical analysis was performed by point-by-point comparison, using a Student's *t*-test (Milligan and Flicker, 1987; Trachtenberg and DeRosier, 1987). Reconstructions were fitted to the atomic resolution model of F-actin (Lorenz et al., 1993), according to the method of McGough and Way (1995), using the program O (Jones et al., 1991), as described by Vibert et al. (1997).

Enzymatic and binding assays

The actin-activated Mg-ATPase rate of unmodified myosin S-1 was measured as previously described (Lin et al., 1996). The Mg-ATPase of the NEM S-1 was low and under all conditions was less than 5% of the measured rate of unmodified S-1. Binding of NEM S-1 to thin filaments was assessed by monitoring cosedimentation of label with actin (Hill et al., 1992). There was no detectable sedimentation of NEM S-1 in the absence of actin.

Binding of myosin S-1·ADP to thin filaments was examined by serial addition of S-1·ADP to samples of thin filaments containing pyrene-labeled actin, as described by Criddle et al. (1985), using an SLM 8000 spectrophotometer and excitation and emission wavelengths of 368 and 407 nm, respectively. Saturating concentrations of S-1 decreased the fluoresence intensity by 79%. Data were corrected for dilution, normalized, and analyzed with the *Scientist* curve-fitting program (MicroMath).

RESULTS AND ANALYSIS

Electron microscopy of reconstituted thin filaments containing D234 tropomyosin and troponin

F-actin was combined with D234 tropomyosin and wild-type cardiac troponin under conditions that saturate filaments with the regulatory proteins to yield a binding of 1 tropomyosin:1 troponin:4 actin expected for filaments with a mutant tropomyosin containing four of the seven tropomyosin repeating regions (see Materials and Methods; cf. Landis et al., 1997, 1999); troponin-D234 tropomyosin bound to actin with an affinity of 4.2 and 2.5×10^6 M^{-1} in the absence and presence of Ca^{2+}, respectively. Electron micrographs of negatively stained reconstituted filaments containing D234 tropomyosin and troponin showed typical actin subunit substructure and occasional elongated strands, characteristic of thin filaments containing tropomyosin (Fig. 1; cf. Lehman et al., 1994, 1995; Vibert et al., 1993, 1997). However, regularly repeating actin helices with a 36-nm-long pitch were not always easily discerned in these filaments, probably because of interference arising from the shorter, out-of-register troponin-tropomyosin period (~22 nm).

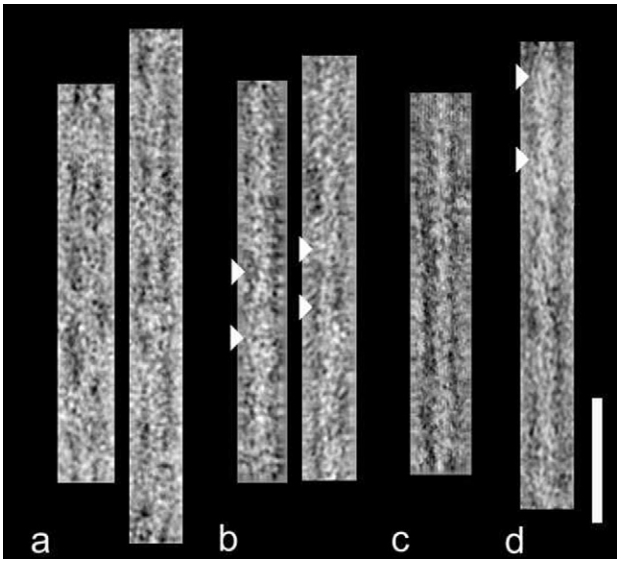

FIGURE 1 Electron micrographs of negatively stained F-actin-tropomyosin-troponin and F-actin-tropomyosin complexes. (*a*) EGTA- and (*b*) Ca^{2+}-treated F-actin-D234 tropomyosin-troponin filaments. (*c*) Troponin-free F-actin-D234 tropomyosin. (*d*) Troponin-free F-actin-skeletal muscle tropomyosin control. Note increased diameter of the filaments containing troponin; also note the tropomyosin strands (*arrowheads*). The scale bar represents 50 nm.

3-D reconstruction of reconstituted thin filaments containing D234 tropomyosin and troponin

Density maps of reconstituted filaments (Figs. 2 and 3, Table 1) were calculated from the averages of Fourier transform layer-line data obtained from the negatively stained filaments. Reconstructions of negatively stained filaments containing D234 and troponin displayed typical two-domain actin monomers that could be further divided into subdomains. Monomer-monomer connectivity was also comparable to that of wild-type thin filaments (cf. Milligan et al., 1990; Vibert et al., 1993, 1997; Lehman et al., 1994, 1995). When compared to maps generated from pure F-actin controls (Figs. 2 and 3), reconstructions of filaments containing D234 showed obvious extra densities indistinguishable from those previously obtained for native and reconstituted filaments containing wild-type tropomyosin (Milligan et al., 1990; Vibert et al., 1993, 1997; Lehman et al., 1994, 1995; Xu et al., 1999). The extra densities were clearly derived from tropomyosin, because they formed characteristic longitudinally continuous strands that appeared the same as those found in reconstructions of filaments lacking troponin (the components of the troponin complex are not resolved by the techniques employed; cf. Milligan and Flicker, 1987). In reconstructions of D234 filaments maintained in EGTA, tropomyosin followed the inner edges of the outer domains of actin (Figs. 2 and 3). It was linked to subdomain 1 and bridged over subdomain 2 of each actin monomer before connecting to subdomain 1 of the axially adjacent monomer (Fig. 2). In the Ca^{2+}-treated filaments, D234 tropomyosin was located on the extreme outer edges of the inner actin domain (Figs. 2 and 3) and connected neighboring monomers by contacts with subdomain 3. The change in position of D234 tropomyosin on actin is comparable to that observed in Ca^{2+}-treated filaments containing wild-type tropomyosin (cf. Lehman et al., 1994; Vibert et al., 1997; Xu et al., 1999).

3-D reconstruction of troponin-free filaments

Inhibition by D234 might be due in principle to the high stoichiometry of troponin on filaments limiting access of myosin to actin-binding sites. However, this is unlikely because, even in the absence of troponin, D234 tropomyosin strongly inhibits motility in vitro (cf. Landis et al., 1997). To better understand D234 inhibition, it was of interest to determine the binding position of D234 in isolation on troponin-free actin. Reconstructions of filaments consisting only of F-actin and D234 (Fig. 1 *c*) showed tropomyosin strands on the inner domain of actin (Fig. 2), i.e., in the position described for the Ca^{2+}-treated filaments above. Hence tropomyosin alone inhibits actomyosin interactions despite being in the "Ca^{2+}-induced" position. Control, non-inhibiting filaments composed of F-actin complexed with wild-type skeletal muscle tropomyosin (Fig. 1 *d*) also showed tropomyosin in this position (Fig. 2), reinforcing the view that the D234 mutant inhibits because it is trapped in the Ca^{2+}-induced position.

The Ca^{2+}-induced position of D234 tropomyosin

To definitively demonstrate that D234 tropomyosin was localized on the inner domain of actin in Ca^{2+}-treated, troponin-containing filaments, the densities attributable to it were determined by subtracting maps of F-actin from maps of actin-D234 filaments. This clearly delineated the boundaries of D234 tropomyosin, and superimposition of the difference densities on the map of pure F-actin confirmed the D234 location on the inner domain of actin (Fig. 4). The difference densities due to mutant tropomyosin were significant at confidence levels greater than 99.95%. Comparison of the position of D234 and wild-type skeletal muscle tropomyosin on troponin-free F-actin showed no notable distinctions (Fig. 4), confirming the location and identity of D234 (cf. Lorenz et al., 1995).

To further define the position of D234 in the Ca^{2+}-induced state at near-atomic resolution, the atomic model of F-actin (Lorenz et al., 1993) was fitted within the envelopes defined by our reconstructions. This process also defined the position of the tropomyosin difference densities determined above, which were then superimposed on the atomic model of actin (Fig. 5). This fitting showed that the D234 tropomyosin (*red wire cage*) occupied positions on actin

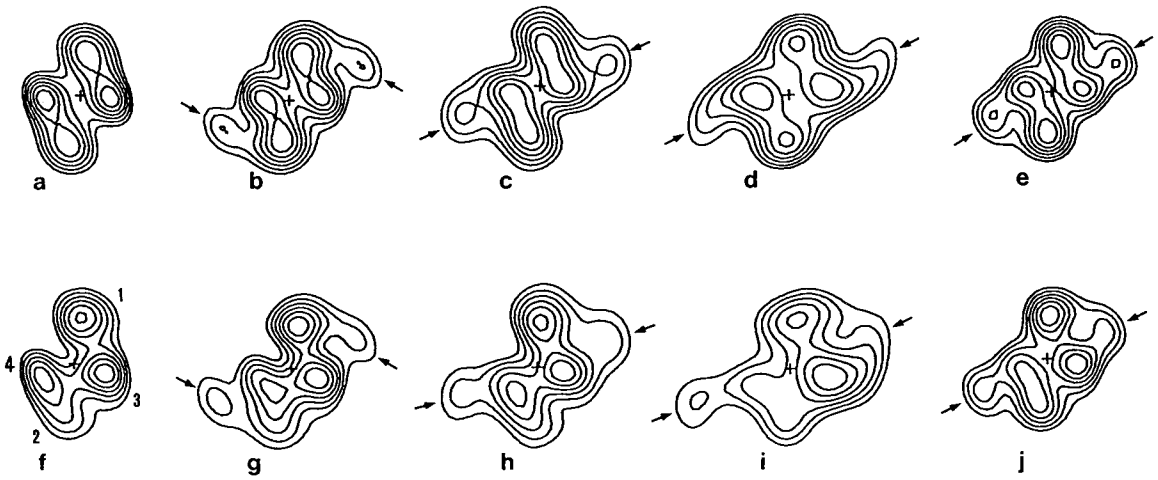

FIGURE 2 Helical projections (*a–e*) and transverse sections (z-sections) (*f–j*) of maps of 3-D reconstructions of negatively stained thin filaments. Helical projections were formed by projecting component densities down the long-pitch actin helices (i.e., along the $n = 2$ helical tracks) onto a plane perpendicular to the thin filament axis; hence the resulting projections show axially averaged positions of tropomyosin relative to actin made bilaterally symmetrical. In contrast, the transverse sections show the position of tropomyosin at a given level along filaments and connectivity to specific subdomains of actin. Because adjacent actin monomers on either side of the filament axis are staggered, sectioning through the center of actin subdomains 1 and 3 of one actin monomer results in sectioning through subdomains 2 and 4 of the other. (*a, f*) F-actin control; subdomains 1–4 are labeled. (*b, g*) EGTA-treated F-actin-D234 tropomyosin-troponin. Note the extra density (*arrows*) associated with subdomains 1 and 2, i.e., on the outer domains of actin monomers. (*c, h*) Ca^{2+}-treated F-actin-D234 tropomyosin-troponin. Note the extra density associated with subdomains 3 and 4, i.e., on the inner domain of actin. Troponin-free filaments containing D234 (*d, i*) and control skeletal muscle (*e, j*) tropomyosin are also shown as paired helical projections and transverse sections. Tropomyosin densities in both are associated with the inner domain of actin. Sections shown are at the same relative axial position along respective reconstructions and projections, and sections all have the same orientation.

(*lavender α-carbon ribbon*), which exposed most clusters of amino acids thought to be involved in strong myosin binding (*highlighted in yellow*; cf. Rayment et al., 1993; Lehman et al., 1995; Vibert et al., 1997). However, one group (including residues 332–334) at the junction of actin subdomains 1 and 3 remained blocked by D234 tropomyosin, thereby occluding the region on subdomain 3, where the tip of the myosin head is located, once it is bound to actin. The same partial unmasking of the myosin-docking region of actin was previously seen in thin filaments with wild-type tropomyosin after Ca^{2+} treatment (Lehman et al., 1994; Vibert et al., 1997; Xu et al., 1999).

NEM S-1-treated filaments

If D234 tropomyosin is inhibitory because it is trapped in the Ca^{2+}-induced position and fails to undergo myosin-induced movement on actin, then it should be possible to reverse the inhibition experimentally by manipulating its position. NEM S-1 binds tightly to actin, even in the presence of ATP, and it activates thin filaments that are inhibited by Ca^{2+}-free wild-type troponin-tropomyosin (Pemrick and Weber, 1976; Williams et al., 1988). Therefore, addition of NEM S-1 to mutant thin filaments was considered a possible way to cause myosin-induced movement and to overcome inhibition by D234. To quantitatively test whether NEM S-1 bound to our filament preparations and would be effective, ^{14}C-labeled NEM S-1 was used to measure interaction by cosedimentation. Tight, saturable binding was observed in the presence of ATP in all samples tested, whether Ca^{2+} was present or not (data not shown). NEM S-1-treated filaments were not used for electron microscopy and image reconstruction because unbound and aggregated material present in such preparations resulted in a high background interference that obscured thin filament fine structure.

In controls and in filaments containing D234, the thin filament-activated Mg-ATPase rate of unmodified S-1 was increased by the addition of NEM S-1 (Fig. 6). As higher concentrations of NEM S-1 were added, the unmodified S-1 ATPase decreased, presumably because free actin sites were filled by NEM S-1 (Fig. 6 and implied by independently measured saturation binding of NEM S-1 on actin). Corrected for the reduced apparent actin concentration, the rates were high on the remaining free actin (analysis not shown). In controls and in samples with very low NEM S-1, the rates were markedly lower for the D234 tropomyosin filaments (Fig. 6, *triangles*) than for filaments with full-length tropomyosin (*circles, squares*). This effect, observed in both the presence and absence of Ca^{2+} (*filled, unfilled symbols*), confirmed that D234 causes Ca^{2+}-independent inhibition. However, inhibition by D234 tropomyosin was largely reversed by NEM S-1, so that the Mg-ATPase rates were similar to those of control filaments in either Ca^{2+} (at ≥ 1.5 μM NEM S-1) or EGTA (at ≥ 3 μM NEM S-1). Because NEM S-1 greatly increased the acto-S-1 ATPase of these

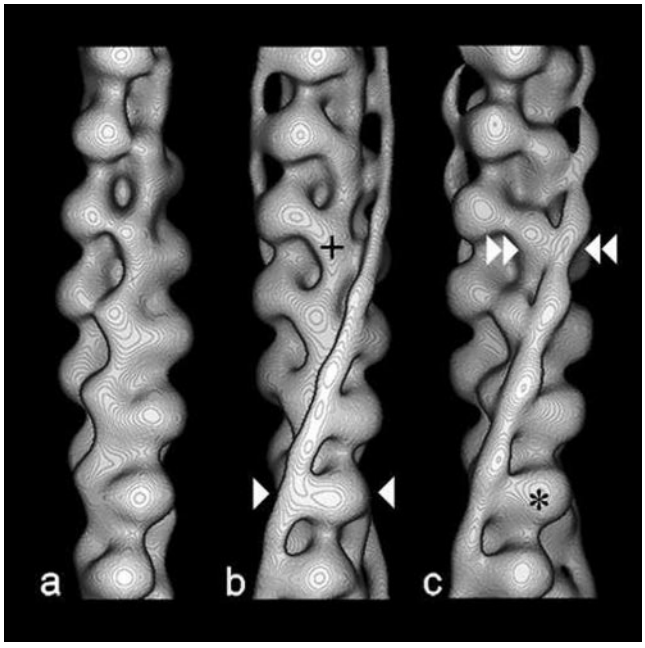

FIGURE 3 Surface views of reconstructions of thin filaments showing the positions of tropomyosin strands superimposed on actin. (*a)* F-actin control. (*b, c*) EGTA- and Ca^{2+}-treated F-actin-D234 tropomyosin-troponin, respectively. In EGTA (*b*), tropomyosin is associated with the inner edge of the outer actin domain of actin. Note the interaction of tropomyosin with actin subdomain 1 (*single white arrowheads*) and bridge of density over the neighboring subdomain 2, while subdomains 3 and 4 remain unobstructed (*black cross*). After Ca^{2+} treatment (*c*), tropomyosin is associated with the outer edge of the inner actin domain of actin. Note that tropomyosin now interacts with subdomain 3 (*double white arrowheads*) while bridging over subdomain 4 and that here subdomains 1 and 2 (*black asterisk*) are unobstructed.

filaments, it appears that bound cross-bridges do reverse the D234 effect, indicating that the inhibitory properties of the mutant tropomyosin are due to impaired switching from the Ca^{2+} state to the fully active "open" state of the thin filament.

Binding of myosin S-1·ADP to thin filaments

The likelihood that D234 inhibition of actomyosin ATPase was due to diminished strong binding of unmodified S-1·nucleotide complexes was not directly assessed by the above analysis but was evaluated by measurements of equilibrium binding of S-1·ADP to actin-tropomyosin-troponin filaments in the presence of calcium. (S-1·ADP was used because it binds tightly and cooperatively to actin-tropomyosin filaments, whereas neither S-1·ATP nor S-1·ADP·P_i does.) To measure this binding, the fluorescence intensity of actin labeled with pyrene on Cys^{374} was monitored as increasing concentrations of S-1·ADP were added (Fig. 7). These results showed weaker binding of S-1·ADP to D234-containing filaments (Fig. 7, *triangles*) than to filaments containing either control cardiac (Fig 7, *squares*) or full-length recombinant tropomyosin (data not shown). Moreover, the binding to D234 tropomyosin filaments was much more cooperative, demonstrated by a particularly low affinity of S-1·ADP for thin filaments containing few bound S-1 molecules. This greater cooperativity may explain why filaments with mutant tropomyosin required more bound NEM S-1 to achieve activation (Fig. 6), because S-1 may be more clustered on actin and hence fewer tropomyosin units may be activated. Filaments containing actin and no regulatory proteins (Fig. 7, *circles*) exhibited weaker S-1·ADP binding than filaments with troponin and either mutant or control tropomyosin.

TABLE 1 Summary of parameters used in image analysis

Sample	*n*	Ψ	ΔΨ	Significance*
EGTA-treated actin-D234 tropomyosin-troponin	9	55.0 ± 4.7°	28.7 ± 4.5°	>99.95%
Ca^{2+}-treated actin-D234 tropomyosin-troponin	16	51.7 ± 6.5°	26.9 ± 7.8°	>99.95%
Troponin-free actin-D234 tropomyosin	7	57.6 ± 4.5°	23.3 ± 6.4°	>99.95%
Troponin-free actin-skeletal muscle tropomyosin	14	55.0 ± 6.5°	26.5 ± 8.7°	>99.95%

n, Number of filaments averaged to generate layer-line data sets and reconstructions.
Ψ, Average phase residual (degrees) ± standard deviation between individual filament layer-line data sets and the average of the data, a measure of the accuracy of the filament alignment.
ΔΨ, Average up-down phase residuals (degrees) ± standard deviation of individual layer-line data sets, a measure of filament polarity.
*The statistical accuracy (confidence level) of tropomyosin densities in reconstructions contoured to 1.8–2.0 nm. All actin densities shown are of comparable or even greater statistical significance.

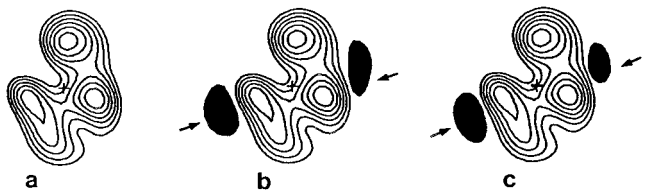

FIGURE 4 Tropomyosin difference density analysis. The locations of tropomyosin densities were determined by subtracting the map of F-actin (*a*) from those of F-actin-tropomyosin complexes and superimposing the resulting difference densities (*filled black*) on the actin map (*b, c*). This process clearly delineates tropomyosin and was used to compare tropomyosin from maps of (*b*) Ca^{2+}-treated F-actin-D234 tropomyosin-troponin and (*c*) control F-actin-skeletal muscle tropomyosin. Note that the positions of tropomyosin (*arrows*), at high levels of statistical significance (Table 1), are the same in each and the same as in previously analyzed Ca^{2+}-treated filaments reconstituted from wild-type tropomyosin-troponin (Xu et al., 1999).

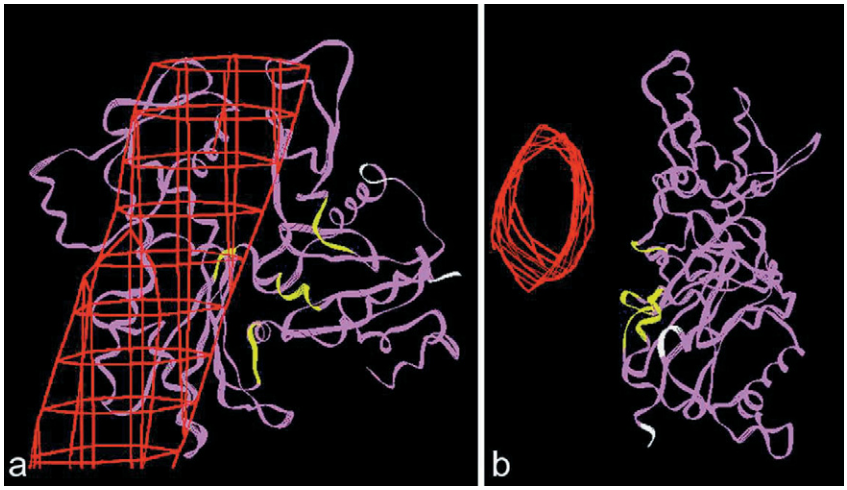

FIGURE 5 Location of D234 tropomyosin densities on the atomic structure of F-actin. Here the atomic model of F-actin (Lorenz et al., 1993) was fitted to our EM reconstruction of Ca^{2+}-treated F-actin-D234 tropomyosin-troponin. A single actin monomer from the atomic model was then substituted for actin in our EM maps; only tropomyosin difference densities are displayed. (*a*) Face-on view (*b*) top view (seen from the pointed end) of actin, showing the amino acid α-carbon chain (*lavender*) with tropomyosin densities (*red*) superimposed. Note that all sites of strong myosin interaction (*highlighted in yellow*) are exposed, with the exception of amino acid residues 332–334 at the junction between subdomains 1 and 3 (cf. Rayment et al., 1993; Holmes, 1995). Other studies on Ca^{2+}-treated wild-type thin filaments (Vibert et al., 1997; Xu et al., 1999) showed a similar partial obstruction of myosin-binding sites. Sites of ionic strength-dependent weak interactions of myosin on the periphery of actin are highlighted in white for reference.

Kinetic analysis of the effects of D234 tropomyosin on thin filament activation

The above binding of S-1·ADP on thin filaments in Ca^{2+} was analyzed according to the 1980 Hill model for cooperative myosin binding to regulated filaments (Hill et al., 1980). In this model, each actin-tropomyosin regulatory unit is considered to be in either a relatively strong or a much weaker myosin-binding state. Although the modeling is independent of a specific structural interpretation, we suggest that the respective states should correspond to conformations of thin filaments with tropomyosin in Ca^{2+}- or myosin-induced positions (Vibert et al., 1997). Tropomyosin's position before Ca^{2+} addition, on the actin outer domain, is not considered in this analysis.

The tropomyosin mutation weakened strong myosin-actin binding, even when the filament was nearly saturated with bound cross-bridges, as is apparent when comparing the upper portions of the plots in Fig. 7. This is reflected by about a twofold change in what we have denoted as K_{strong}, the parameter that measures strong myosin binding in the Hill model. (Hill named this parameter K_2, a term we use below in a different sense.) Calculations using the Hill model indicated that the increased cooperativity displayed by the D234 tropomyosin filaments is mostly attributable to a 3.5-fold increase in the equilibrium constant L'. L' is similar to $1/K_T$ in the McKillop and Geeves model (1993) and is a measure of the "open" to "closed" thin filament conformational transition in the absence of myosin. The degree of cooperativity in the calculated binding curves was less sensitive to the change from seven to four actins in a regulatory unit and to a tropomyosin-tropomyosin interaction parameter Y (cf. Williams and Greene, 1983).

DISCUSSION

In the current study, we uncoupled Ca^{2+}- and myosin-induced tropomyosin movement on thin filaments, using a tropomyosin deletion mutant, D234, preventing activation of myosin ATPase by the filaments. The observation that Ca^{2+}-induced movement of tropomyosin alone is insufficient to turn on thin filaments and that further movement caused by myosin is essential demonstrates that tropomyosin is not simply part of a two-state on-off switching mechanism governed only by Ca^{2+} binding to troponin. In contrast, the data strongly support the three-state model of regulation in which activation is considered to be a stepwise process involving sequential Ca^{2+}- and myosin-induced transitions releasing inhibition (cf. Vibert et al., 1997). Furthermore, the results indicate that the Ca^{2+}-induced state is not an active state that is merely unpotentiated. Rather, the Ca^{2+} state remains switched off by being relatively "closed" to myosin binding (cf. Lehrer and Geeves, 1998).

Tropomyosin is characterized by two distinct repeating patterns of amino acids. At one level of organization, heptad repeats cause coiled-coil formation and tropomyosin dimerization. At the other, quasi-repeating sequences are thought to be responsible for actin binding (McLachlan and Stewart, 1976; Phillips et al., 1986). Unraveling the structural and functional consequences of substituting deletion mutants for wild-type tropomyosin in thin filaments should help to

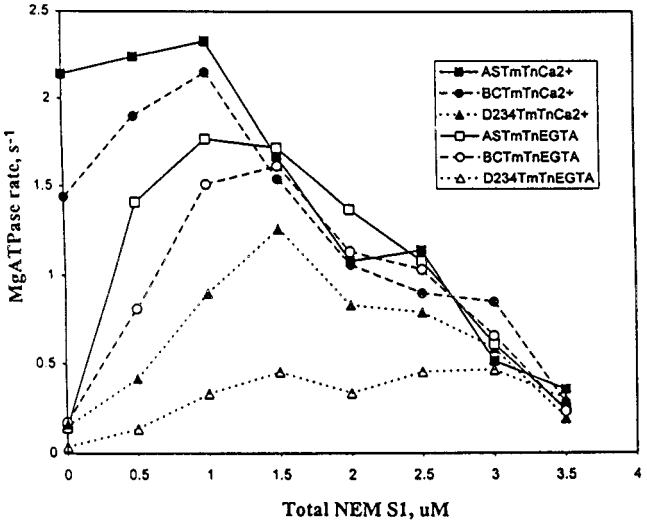

FIGURE 6 Effect of NEM S-1 on thin filament-activated Mg-ATPase activity of unmodified S-1. Shown are average data points from two experiments each for three types of thin filaments, measured in the presence and absence of Ca^{2+} and containing troponin (Tn) and D234 tropomyosin (△, ▲), recombinant full-length tropomyosin (ASTm, □, ■) (Landis et al., 1997), or tropomyosin isolated from bovine cardiac muscle (BCTm, ○, ●). ●, ■, ▲, 0.1 mM $CaCl_2$; ○, □, △, 0.5 mM EGTA. Conditions: 25 mM KCl, 10 mM NaH_2PO_4, 1 mM ATP, 3.5 mM $MgCl_2$, 3.5 μM F-actin, and either 0.9 μM troponin and 0.8 μM full-length tropomyosin or 1.6 μM troponin and 1.5 μM D234 tropomyosin. These concentrations of regulatory proteins are sufficient to saturate the actin (Landis et al., 1997). Unmodified myosin S-1 (1 μM) was added to all samples, and NEM S-1 was varied as indicated. The curves are biphasic because NEM S-1 first potentiates the ATPase activity but then decreases it by progressively blocking more myosin binding sites on actin. Note that NEM S-1 increases the Mg-ATPase activity for all samples tested, but more NEM S-1 is required to potentiate thin filaments containing D234 than normal tropomyosin. For any given sample type, the rank order of the ATPase rates shown was consistent for each of the 16 assays performed in either the presence or absence of Ca^{2+} at all NEM S-1 concentrations tested. The respective relative magnitudes of ATPase values between different types of samples were also consistent.

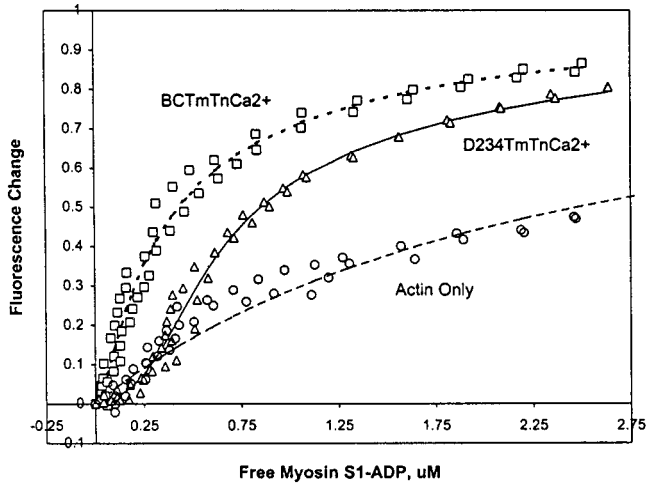

FIGURE 7 Binding of myosin S-1·ADP to thin filaments in Ca^{2+}. Compared to thin filaments with wild-type cardiac tropomyosin (BCTm, □), filaments with D234 tropomyosin (△) had weakened myosin S-1·ADP binding and increased cooperativity. However, S-1·ADP binding to D234 filaments was still tighter than S-1·ADP binding to tropomyosin-free F-actin (○). A hyperbolic binding curve was fitted to the data on F-actin, using a *Scientist* curve-fitting algorithm. Binding curves for data on F-actin-tropomyosin-troponin were generated as dictated by the cooperative binding model of Hill et al. (1980). Calculations were appropriately modified for D234 filaments to adjust for their short regulatory unit. These procedures also defined the following parameters (terms specified in the text): actin, $K = 4.0 \pm 0.1 \times 10^5\ M^{-1}$; actin-troponin-cardiac tropomyosin, $K_{weak} = 10\ M^{-1}$, $K_{strong} = 2.37 \pm 0.16 \times 10^6\ M^{-1}$, $L' = 1.8 \pm 1$, $Y = 1.5$; actin-troponin-D234, $K_{weak} = 10\ M^{-1}$, $K_{strong} = 1.47 \pm 0.08 \times 10^6\ M^{-1}$, $L' = 6.1 \pm 0.8$, $Y = 2.9$. Conditions: 25°C, 200 mM KCl, 3 mM $MgCl_2$, 20 mM imidazole (pH 7.5), 0.2 mM ADP, 10 μM P_1, P_5-di(adenosine-5′)pentaphosphate (an inhibitor of myokinase), 0.5 mM glucose, 6 units/ml hexokinase, 0.1 mM $CaCl_2$, 2.5 μM actin, and 1.3 μM of either tropomyosin-troponin or D234-troponin. Similar results were obtained in the presence of 2 mM ADP under otherwise identical conditions (data not shown).

further elucidate their mechanism of activation. Emerging evidence demonstrates that deleting quasi-repeating modules hardly weakens actin-tropomyosin interaction (Hitchcock-DeGregori and Varnell, 1990; Hitchcock-DeGregori and An, 1996; Landis et al., 1997, 1999). For example, differences in D234 and control tropomyosin binding to myosin-free actin are small, and, in addition, the D234 deletion had no weakening effect on troponin-tropomyosin binding to myosin-free actin, in the presence or in the absence of calcium (Landis et al., 1997). Similar results were found previously for deletions of regions 2 and 3 (Hitchcock-DeGregori and An, 1996; cf. Landis et al., 1999). In contrast, the strongly enhanced actin-tropomyosin binding in the presence of myosin S-1 is considerably influenced by such deletions (Landis et al., 1997, 1999). Here, for example, the D234 tropomyosin mutant binds to acto-myosin S-1 at least 100 times more weakly than does control tropomyosin (Landis et al., 1997). What we have now shown is that deletion of specific regions of tropomyosin affects not only aspects of actin binding but also conformational switching of the thin filament to its active state.

It is thought that tropomyosin in the Ca^{2+}-induced state sterically blocks part of the myosin-binding site on actin (Vibert et al., 1997). However, were binding of tropomyosin and myosin strictly competitive, then myosin S-1 would be expected to weaken association of tropomyosin with thin filaments, contrary to observation. In fact, the affinity of wild-type tropomyosin for myosin-decorated actin is extremely high (cf. Eaton, 1976; Cassell and Tobacman, 1996), and this must be taken into account when considering the myosin-induced movement of tropomyosin beyond its position in the Ca^{2+}-induced state. To explain the tight binding, myosin might bind directly to tropomyosin. Although there is no evidence for interaction of tropomyosin and myosin in solution, the proximity of tropomyosin and

S-1 in decorated filaments still allows for such a possibility (cf. Milligan et al., 1990; Vibert et al., 1997). Alternatively, myosin might allosterically enhance tropomyosin binding by causing a conformational change in actin linked to activation. Presumably, this, in turn, would further enhance myosin binding. The possibility of such a conformational change occurring is suggested by the large 100-fold or greater increase in tropomyosin affinity for actin accompanying S-1 binding (Cassell and Tobacman, 1996; Landis et al., 1997) and by the corresponding increase in S-1 binding after tropomyosin association (Fig. 7). Regardless of whether the reciprocally enhanced tropomyosin and myosin binding is direct or mediated through actin, the process must be linked energetically. In our studies, we have broken this energy-coupled linkage by substituting mutant for wild-type tropomyosin (Fig. 7 and Landis et al., 1997), resulting in tropomyosin poorly enhancing myosin binding and, likewise, myosin poorly increasing tropomyosin binding. We recognize that the molecular nature of transitions of myosin on actin, e.g., from weak to strong binding, are not well understood, but suggest that they are intimately controlled by the Ca^{2+}- and myosin-induced effects on tropomyosin. Therefore, it is not surprising that specific deletion of tropomyosin repeats perturbs the progression of events during the cooperative activation of the thin filament orchestrated by both tropomyosin and myosin.

We propose that the tight binding of myosin to actin requires tropomyosin to adopt a position on actin that is energetically unfavorable unless actin undergoes a conformational change. The D234 mutation would inhibit the tropomyosin transition and myosin-induced actin conformational change, perhaps because of the binding of only four instead of the normal seven tropomyosin sites to actomyosin. In this model, tropomyosin has both steric and allosteric roles. It sterically blocks myosin binding but allosterically promotes a thin-filament conformational change that occurs when myosin is bound to actin. In addition to myosin's obvious enzymatic and motor roles, it also acts as an allosteric effector coupled energetically to the allostery of tropomyosin. These two linked allosteric processes lead cooperatively to the open state of the filament (McKillop and Geeves, 1993), i.e., to what traditionally was called "potentiation" (Bremel et al., 1972). Among the unresolved issues suggested by this model are the nature of the possible

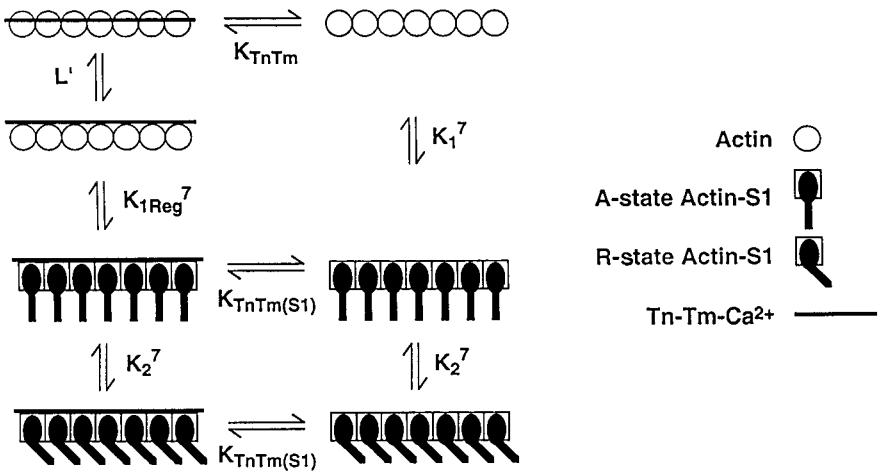

FIGURE 8 Schematic model of myosin and troponin-tropomyosin binding to actin in Ca^{2+}. Tropomyosin-free actin is depicted as seven contiguous circles and tropomyosin-troponin as a longitudinally oriented bar in contact with identically drawn actin. The A- to R-state transition is represented as a reorientation of the myosin regulatory domains on actin. For consistency, closed and open positions of tropomyosin on actin are illustrated as in McKillop and Geeves (1993); the blocked configuration does not enter into our modeling of Ca^{2+}-treated filaments. Myosin S-1 binds to tropomyosin-free actin in at least two steps, characterized by K_1 and K_2 with $K_2 \gg 1$, resulting in formation of weak (A-state) and then strong (R-state) bonds. For Ca^{2+}-saturated troponin-tropomyosin (TnTm), the first of these steps, K_{1Reg}, occurs with fourfold to sevenfold higher affinity than that for actin alone (K_1) such that $K_{1Reg}^7 \gg K_1^7$ (with the exponent, 7, accounting for regulatory units of seven actin monomers, maximally occupied by seven S-1 heads). However, the A- to R-state isomerization (K_2) itself is unaffected by TnTm (Geeves and Halsall, 1986). Therefore the product $K_{1Reg}K_2$ (corresponding to K_{strong} in Fig. 7) is greater than K_1K_2 (cf. Murray et al., 1982; Williams and Greene, 1983). We propose that the increased S-1 binding to TnTm-actin in the A-state requires an azimuthal movement of tropomyosin beyond its Ca^{2+}-induced position and a conformational change in actin coupled to the myosin binding and tropomyosin movement. The equilibrium linkage relationships illustrated imply that the regulatory proteins bind tightly to both A-state and R-state acto-S-1; i.e., $K_{TnTm(S1)} \gg K_{TnTm}$ energetically balances $K_{1Reg}^7 \gg K_1^7$, because $K_{TnTm(S1)} \cdot K_1^7 \sim K_{TnTm} \cdot K_{1Reg}^7$ (corresponding experimental support found in Eaton (1976), Szczesna et al. (1989), Cassell and Tobacman (1996), and Landis et al. (1997)). We have not considered here the ionic strength-dependent, weak binding of myosin S-1·ATP to actin (Miller et al., 1995), which is not thought to depend on the azimuthal position of tropomyosin in any of the states described (cf. Holmes, 1995; Vibert et al., 1997). The equilibrium linkage scheme that we have modeled is based on data obtained with high myosin binding density on thin filaments and dominated by the combined binding energies of multiple myosin heads in each regulatory unit. We have not been able to differentiate between events occurring during the binding of the first myosin S-1 to regulatory units and those accompanying binding of subsequent S-1 molecules. Moreover, our modeling has not determined whether or not tropomyosin movement to an "open" state precedes or follows initial S-1 binding.

conformational change in actin induced by myosin and regulatory proteins and how it is related to enhancement of actin-myosin interactions. Whether the proposed change in actin is a result of local alterations in charged surface residues or a larger conformational change is not known. The participation of various regions of tropomyosin in this process is being examined with the aid of other deletion mutants, and their relationship to cross-bridge function on regulated thin filaments is being tested.

Kinetic analysis of Geeves and co-workers (Coates et al., 1985) indicated that after an initial collision complex, myosin S-1 associates with actin weakly (K_1), forming the so-called A-state of myosin, and then isomerizes ($K_2 \gg 1$) to form the stronger R-state (see Fig. 8). The formalism was later expanded to include regulatory states, viz. the "blocked" off state of thin filaments, in which Ca^{2+}-free troponin-tropomyosin prevents myosin binding, and "closed" and "open" states formed in the presence of Ca^{2+} (McKillop and Geeves, 1993). The latter correspond to states capable of weak and strong thin-filament–S-1 binding during the transition to the R-state. A model for myosin binding to Ca^{2+}-saturated thin filaments is schematically shown in Fig. 8; it incorporates previously published information (cf. Lehrer and Geeves, 1998) and our new data. The equilibrium between open and closed states of S-1 free filaments is represented by L' and initial weak binding of S-1 and isomerization to strong binding as K^7_{1Reg} and K^7_2, respectively. Troponin-tropomyosin in the presence of Ca^{2+} (or tropomyosin alone $\pm$ Ca^{2+}) increases the affinity of myosin S-1 for actin (Fig. 7 and Murray et al., 1982; Williams and Greene, 1983) because $K_{1Reg} > K_1$; however, the subsequent A- to R-state isomerization (K_2) is considered to be unaffected by troponin-tropomyosin (Geeves and Halsall, 1986). As illustrated in the model in Fig. 8, it follows that if the A- to R-state equilibrium is not changed by troponin-tropomyosin, then tight binding of the regulatory proteins must be promoted by A-state and not just by R-state myosin. Hence we conclude that cooperative interactions between tropomyosin and bound myosin heads occur before the A- to R-state transition. This cooperativity is presumably dependent on tropomyosin position, and, we suggest, A-state binding of myosin is promoted as the open state forms. In addition, we propose that acto-tropomyosin-S-1 differs conformationally from tropomyosin-free acto-S-1, and that the new conformation formed cooperatively promotes enhanced myosin binding, leading to full activation in the R-state. D234 tropomyosin influences L', favoring a closed position of tropomyosin and hence inhibiting A-state S-1 binding. By disrupting the newly described conformational change, D234 also weakens S-1 binding after any tropomyosin movement to the open state. Our model provides a plausible synthesis of 1) the binding of normal and mutant regulatory proteins to actin and acto-S-1, 2) previously modeled equilibria and kinetics of thin filament-S-1 interactions, and 3) structural information on myosin and tropomyosin positions in thin filaments during activation.

The authors thank Earl Homsher and Victoria Hatch for critically reading the manuscript. We are grateful to N. Gherbesi for assistance with photography.

This work was funded by National Institutes of Health Research grants HL36153 (to WL), AR34711 (to RC), and HL38834 (to LST) and a National Institutes of Health Shared Instrumentation grant RR08426 (to RC) supporting electron microscope facilities.

REFERENCES

Amos, L. A., and A. Klug. 1975. Three-dimensional image reconstruction of the contractile tail of T4 bacteriophage. *J. Mol. Biol.* 99:51–73.

Bremel, R. D., J. M. Murray, and A. Weber. 1972. Manifestations of cooperative behavior in the regulated actin filament during actin-activated ATP hydrolysis in the presence of calcium. *Cold Spring Harb. Symp. Quant. Biol.* 37:267–275.

Cassell, M., and L. S. Tobacman. 1996. Opposite effects of myosin subfragment 1 on binding of cardiac troponin and tropomyosin to the thin filament. *J. Biol. Chem.* 271:12867–12872.

Coates, J. H., A. H. Criddle, and M. A. Geeves. 1985. Pressure-relaxation studies of pyrene-labeled actin and myosin subfragment 1 from rabbit skeletal muscle. Evidence for two states of actin-subfragment 1. *Biochem. J.* 232:351–356.

Cohen, I., and C. Cohen. 1972. A tropomyosin-like protein from human platelets. *J. Mol. Biol.* 68:383–387.

Criddle, A. H., M. A. Geeves, M. A., and T. Jeffries. 1985. The use of actin labeled with *N*-(1-pyrenyl)iodoacetamide to study the interaction of actin with myosin subfragments and troponin/tropomyosin. *Biochem. J.* 232:343–349.

DeRosier, D. J., and P. B. Moore. 1970. Reconstruction of three-dimensional images from electron micrographs of structures with helical symmetry. *J. Mol. Biol.* 52:355–369.

Eaton, B. L. 1976. Tropomyosin binding to F-actin induced by myosin heads. *Science.* 192:1337–1339.

Egelman, E. H. 1986. An algorithm for straightening images of curved filamentous structures. *Ultramicroscopy.* 19:367–374.

Flicker, P. F., G. N. Phillips, and C. Cohen. 1982. Troponin and its interactions with tropomyosin. An electron microscope study. *J. Mol. Biol.* 162:495–501.

Geeves, M. A., and D. J. Halsall. 1986. The dynamics of the interaction between myosin subfragment 1 and pyrene-labeled thin filaments from rabbit skeletal muscle. *Proc. R. Soc. Lond. B.* 229:85–95.

Haselgrove, J. C. 1972. X-ray evidence for a conformational change in actin-containing filaments of vertebrate striated muscle. *Cold Spring Harb. Symp. Quant. Biol.* 37:341–352.

Hill, L. E., J. P. Mehegan, C. A. Butters, and L. S. Tobacman. 1992. Analysis of troponin-tropomyosin binding to actin. Troponin does not promote interactions between tropomyosin molecules. *J. Biol. Chem.* 267:16106–16113.

Hill, T. L., E. Eisenberg, and L. E. Greene. 1980. Theoretical model for the cooperative equilibrium binding of myosin subfragment 1 to actin-troponin-tropomyosin complex. *Proc. Natl. Acad. Sci. USA.* 77: 3186–3190.

Hitchcock-DeGregori, S. E., and Y. An. 1996. Integral repeats and a continuous coiled coil are required for binding of striated tropomyosin to the regulated thin filament. *J. Biol. Chem.* 271:3600–3603.

Hitchcock-DeGregori, S. E., and T. A. Varnell. 1990. Tropomyosin has discrete actin binding sites with sevenfold and fourteenfold periodicities. *J. Mol. Biol.* 214:885–896.

Holmes, K. C. 1995. The actomyosin interaction and its control by tropomyosin. *Biophys. J.* 68(Suppl.):2–7.

Huxley, H. E. 1972. Structural changes in actin- and myosin-containing filaments during contraction. *Cold Spring Harb. Symp. Quant. Biol.* 37:361–376.

Jones, T. A., J. Y. Zou, S. W. Cowan, and M. Kjeldgaard. 1991. Improved methods for the building of protein models in electron density maps and the location of errors in these models. *Acta Crystallogr. A.* 47:110–119.

Landis, C. A., N. Back, E. Homsher, and L. S. Tobacman. 1999. Effects of tropomyosin internal deletions on thin filament function. *J. Biol. Chem.* 274:31279–31285.

Landis, C. A., A. Bobkova, E. Homsher, and L. S. Tobacman. 1997. The active state of the thin filament is destabilized by an internal deletion in tropomyosin. *J. Biol. Chem.* 272:14051–14056.

Lehman, W., R. Craig, and P. Vibert. 1994. Ca^{2+}-induced tropomyosin movement in *Limulus* thin filaments revealed by three-dimensional reconstruction. *Nature.* 368:65–67.

Lehman, W., P. Vibert, P. Uman, and R. Craig. 1995. Steric-blocking by tropomyosin visualized in relaxed vertebrate muscle thin filaments. *J. Mol. Biol.* 251:191–196.

Lehrer, S. S. 1994. The regulatory switch of muscle thin filaments. Ca^{2+} or myosin heads? *J. Muscle Res. Cell Motil.* 15:232–236.

Lehrer, S. S., and M. A. Geeves. 1998. The muscle thin filament as a classical cooperative/allosteric regulatory system. *J. Mol. Biol.* 277: 1081–1089.

Lehrer, S. S., and E. P. Morris. 1982. Dual effects of tropomyosin and troponin-tropomyosin on subfragment 1 ATPase. *J. Biol. Chem.* 257: 8073–8080.

Lin, D., A. Bobkova, E. Homsher, and L. S. Tobacman. 1996. Altered cardiac troponin T in vitro function in the presence of a mutation implicated in familial hypertrophic cardiomyopathy. *J. Clin. Invest.* 97:2842–2848.

Lorenz, M., K. J. V. Poole, D. Popp, G. Rosenbaum, and K. C. Holmes. 1995. An atomic model of the unregulated thin filament obtained by x-ray fiber diffraction on oriented actin-tropomyosin gels. *J. Mol. Biol.* 246:108–119.

Lorenz, M., D. Popp, and K. C. Holmes. 1993. Refinement of the F-actin model against x-ray fiber diffraction data by use of a directed mutation algorithm. *J. Mol. Biol.* 234:826–836.

McGough, A., and M. Way. 1995. Molecular model of an actin filament capped by a severing protein. *J. Struct. Biol.* 115:144–150.

McKillop, D. F. A., and M. A. Geeves. 1993. Regulation of the interaction between actin and myosin subfragment-1: evidence for three states of the thin filament. *Biophys. J.* 65:693–701.

McLachlan, A. D., and M. Stewart. 1976. The 14-fold periodicity in α-tropomyosin and the interaction with actin. *J. Mol. Biol.* 103:271–298.

Miller, C. J., P. Cheung, P. White, and E. Reisler. 1995. Actin's view of the actomyosin interface. *Biophys. J.* 68(Suppl.):50–56.

Milligan, R. A., and P. F. Flicker. 1987. Structural relationships of actin, myosin, and tropomyosin revealed by cryo-electron microscopy. *J. Cell Biol.* 105:29–39.

Milligan, R. A., M. Whittaker, and D. Safer. 1990. Molecular structure of F-actin and the location of surface binding sites. *Nature.* 348:217–221.

Monteiro, P. B., R. C. Lataro, J. A. Ferro, and F. C. Reinach. 1994. Functional alpha-tropomyosin produced in *Escherichia coli.* A dipeptide extension can substitute for the amino-terminal acetyl group. *J. Biol. Chem.* 269:10461–10466.

Moody, C., W. Lehman, and R. Craig. 1990. Caldesmon and the structure of vertebrate smooth muscle thin filaments: electron microscopy of isolated thin filaments. *J. Muscle Res. Cell Motil.* 11:176–185.

Murray, J. M., M. K. Knox, C. E. Trueblood, and A. Weber. 1982. Potentiated state of the tropomyosin actin filament and nucleotide-containing myosin subfragment 1. *Biochemistry.* 21:906–915.

Murray, J. M., and A. Weber. 1973. Molecular control mechanisms in muscle contraction. *Physiol. Rev.* 53:612–673.

Owen, C., D. G. Morgan, and D. J. DeRosier. 1996. Image analysis of helical objects: the Brandeis helical package. *J. Struct. Biol.* 116: 167–175.

Parry, D. A. D., and J. M. Squire. 1973. Structural role of tropomyosin in muscle regulation: analysis of x-ray patterns from relaxed and contracting muscles. *J. Mol. Biol.* 75:33–55.

Pemrick, S., and A. Weber. 1976. Mechanism of inhibition by *N*-ethylmaleimide treatment of myosin. *Biochemistry.* 15:5193–5198.

Phillips, G. N., J. P. Fillers, and C. Cohen. 1986. Tropomyosin crystal structure and muscle regulation. *J. Mol. Biol.* 192:111–131.

Poole, K. V. G., G. Evans, G. Rosenbaum, M. Lorenz, and K. C. Holmes. 1995. The effect of cross-bridges on the calcium sensitivity of the structural change of the regulated thin filament. *Biophys. J.* 68:365a (Abstr.).

Rayment, I., H. M. Holden, M. Whittaker, C. B. Yohn, M. Lorenz, K. C. Holmes, and R. A. Milligan. 1993. Structure of the actin-myosin complex and its implications for muscle contraction. *Science.* 261:58–65.

Spudich, J. A., and S. Watt. 1971. The regulation of rabbit skeletal muscle contraction. I. Biochemical studies of the interaction of the tropomyosin-troponin complex with actin and the proteolytic fragments of myosin. *J. Biol. Chem.* 242:4866–4871.

Szczesna, D., Y. S. Borovikov, and A. Sobieszek. 1989. Interaction of tropomyosin with F-actin-heavy meromyosin complex. *Biol. Chem. Hoppe-Seyler.* 370:399–407.

Tobacman, L. S., and R. S. Adelstein. 1986. Mechanism of regulation of cardiac actin-myosin subfragment 1 by troponin-tropomyosin. *Biochemistry.* 25:798–802.

Trachtenberg, S., and D. J. DeRosier. 1987. Three-dimensional structure of the frozen-hydrated flagellar filament: the left-handed filament of *Salmonella typhimurium*. *J. Mol. Biol.* 195:581–601.

Vibert, P., R. Craig, and W. Lehman. 1993. Three-dimensional reconstruction of caldesmon-containing smooth muscle thin filaments. *J. Cell Biol.* 123:313–321.

Vibert, P., R. Craig, and W. Lehman. 1997. Steric-model for activation of muscle thin filaments. *J. Mol. Biol.* 266:8–14.

Weeds, A. G., and R. S. Taylor. 1975. Separation of subfragment-1 isoenzymes from rabbit skeletal muscle myosin. *Nature.* 257:54–56.

Willadsen, K. A., C. A. Butters, L. E. Hill, and L. S. Tobacman. 1992. Effects of the amino-terminal regions of tropomyosin and troponin T on thin filament assembly. *J. Biol. Chem.* 267:23746–23752.

Williams, D. L., and L. E. Greene. 1983. Comparison of the effects of tropomyosin and troponin-tropomyosin on binding of myosin subfragment 1 to actin. *Biochemistry.* 22:2770–2774.

Williams, D. L., L. E. Greene, and E. Eisenberg. 1988. Cooperative turning on of myosin subfragment 1 adenosine triphosphatase activity by the troponin-tropomyosin complex. *Biochemistry.* 27:6987–6993.

Xu, C., R. Craig, L. Tobacman, R. Horowitz, and W. Lehman. 1999. Tropomyosin positions in regulated thin filaments revealed by cryoelectron microscopy. *Biophys. J.* 77:985–992.